Journal of Cleaner Production 246 (2020) 119018

Contents lists available at ScienceDirect

Journal of Cleaner Production

journal homepage: www.elsevier.com/locate/jclepro

How does urban expansion impact people's exposure to green environments? A comparative study of 290 Chinese cities

Yimeng Song [a], Bin Chen [b, *], Mei-Po Kwan [c, d]

[a] Department of Urban Planning and Design, The University of Hong Kong, Pok Fu Lam, Hong Kong
[b] Department of Land, Air and Water Resources, University of California, Davis, CA, 95616-8627, USA
[c] Department of Geography and Resource Management, and Institute of Space and Earth Information Science, The Chinese University of Hong Kong, Shatin, Hong Kong, China
[d] Department of Human Geography and Spatial Planning, Utrecht University, Utrecht, 3584 CB, the Netherlands

ARTICLE INFO

Article history:
Received 16 March 2019
Received in revised form
1 August 2019
Accepted 22 October 2019
Available online 23 October 2019

Handling editor: Xin Tong

Keywords:
Urban greenspace
Urban sprawl
Exposure assessment
Old and new urban area
Human mobility

ABSTRACT

Understanding the difference of greenspace in different urban areas is a critical requirement for maintaining urban natural environment and lessening environmental inequality. However, how urban expansion impacts on people's exposure to ambient green environments has been limitedly addressed. Here we integrated multi-source geospatial big data including mobile-phone location-based service (LBS) data, Sentinel-2, and nighttime light satellite imageries to quantitatively estimate changes in people's exposure to green environments for 290 cities in China from 1992 to 2015. Results showed that the urban expansion process directly led to differences in green environments between old and new urban areas. These differences were not only observed by the green coverage rate but also captured using a dynamic assessment of people's exposure to greenspace. For most of China's large cities, people could enjoy more greenspace in new urban areas than the old ones. A significant day-to-night variation of people's exposure to greenspace was identified between old and new urban areas. Our results also revealed that urbanization did bring some positive effects to improve green environments for cities located in harsh natural conditions (e.g., semiarid/arid and desert regions).

1. Introduction

Urban greenspace, typically including open and undeveloped land with green vegetation such as parks, gardens, street plants, lawns, green roofs, and forests within urban areas (Mitchell and Popham, 2008), is regarded as one of the most important factors in people's living environment. Previous studies have extensively shown that urban greenspaces play a vital role in maintaining environmental quality and alleviating numerous urban problems, such as mitigating noise levels (Van Renterghem and Botteldooren, 2016), absorbing particle air pollutants (Janhäll, 2015), infiltrating stormwater (Livesley et al., 2016), and alleviating the heat island effect (Andersson-Sköld et al., 2015). Besides, urban greenspaces also contribute to promoting residents' activities and social interactions, and improving both physical and mental health (Ernstson, 2013; Wolch et al., 2014).

With rapid global urbanization, hundreds of millions of people have moved into urban areas over the past decades (Lang et al., 2016; Wang et al., 2012). Statistically, the world urbanization rate increased from 30% to more than 50% from 1950 to 2015 (Jiang and O'Neill, 2017) and was estimated to reach 75% in 2050 (Giles-Corti et al., 2016). The dramatic growth of urban population undoubtedly led to urban sprawls worldwide (Gong et al., 2012). For example, during the period 1982–1997, urban areas in 281 American cities increased by 47% (Fulton et al., 2001). A similar phenomenon was also found in Europe, where urban was land increased by 1117.9 km^2 per year from 2000 to 2006 (Hennig et al., 2015). Moreover, urban expansion in China witnessed an average growth rate of 16.32% per year from 1981 to 2010 (Xiao et al., 2014). In addition to quantifying the magnitude of urban expansion, a better assessment of the impact of such processes and the difference they brought to the green environment between old urban areas and newly built urban areas ("new urban areas" hereafter) is urgently needed. However, previous studies addressing these issues are quite limited, and answers about them remain unclear, especially for small and medium cities.

* Corresponding author.
E-mail address: bch@ucdavis.edu (B. Chen).

https://doi.org/10.1016/j.jclepro.2019.119018
0959-6526/

Urbanization is highly linked to the conversion of natural lands to artificial surfaces (He et al., 2014). Some studies pointed out that, with the deepening of urbanization, cities began to face a gradual reduction of greenspaces, which brought great pressure to the living environment (Chen et al., 2017; Grimm et al., 2008). However, does urbanization only have negative impacts upon urban green environments? Also, compared with new urban areas, are highly urbanized old urban areas doomed to have worse green environments? To answer these questions, a more comprehensive study is needed, drawing upon an adequate number of sample cities with diverse physical and socioeconomic characteristics. Generally, the widely used indicators such as green coverage rate (GCR) and greenspace area per capita (GAC), are capable of providing an overall assessment of urban greenspace (Yang et al., 2014; Zhao et al., 2013). Nevertheless, the real experience concerning individuals' ambient green environment during different temporal periods is another more important metric to evaluate the fair or foul of urban greenery in terms of quantity and distribution. In consequence, greenspace assessments that consider human mobility should be applied to receive a better understanding of the greenspace distribution in different urban areas.

High spatially and temporally resolved information has become increasingly important in studies regarding urban environment and public health. Specifically, in urban greenspace assessments, some recently launched satellites equipped with advanced optical sensors have the capability to provide remote sensing images with much higher spatial-temporal resolution (e.g., Sentinel-2) (Zhang et al., 2018). These data significantly improved the accuracy of greenspace mapping. Moreover, the appearing of geospatial big data (e.g., social media data, mobile phone data, and taxi data) provides further opportunities for researchers to uncover the patterns of human mobility and dynamic distribution (Liu et al., 2015). The utilization of these data is also regarded as an effective way to reduce the uncertainty in quantifying the interaction between people and their ambient environment.

By using multi-source geo-spatial big data and improved methods, this study aimed to undertake a comprehensive analysis of urban greenspaces in Chinese cities and answer the following questions: (1) What are the differences in urban greenspace between old and new urban areas in Chinese cities? (2) How do the differences vary when human mobility is considered? (3) What are the impacts (positive or negative) of urbanization upon the green environment of different urban areas? Compared with previous studies concerning greenspace evaluation, this study advanced the literature in several aspects. First, we integrated land cover data and nighttime light images to produce more reasonable urban-area boundaries for greenspace analysis. Second, greenspace mapping with a higher spatial resolution was derived from Sentinel-2 optical images based on a linear spectral unmixing model, thus providing accurate and detailed information about greenspace distribution. Third, human mobility was introduced into greenspace exposure estimation, thereby providing an improved way to understand people' exposure to ambient green environment at different times of the day. Lastly, for the purpose of giving a full picture of the differences among Chineses cities, the proposed methods and assessments were applied to 290 major cities in China.

2. Related works

Currently, some disagreements can be identified in existing studies that examine urban greenspaces, and most of them are mainly due to the differences in semantic definitions (Chen et al., 2017). In some studies, urban greenspace was narrowly defined as outdoor places with significant amounts of vegetation (Jim and Chen, 2003), or only some particular categories of land (e.g., public parks or open gardens) were taken into account (Akpinar, 2016; Kong et al., 2007). Generally, urban greenspace was defined as land with vegetation cover and has diverse characteristics, varying sizes, and different species richness (Fuller and Gaston, 2009; Sister et al., 2010), including but not limited to parks, sporting fields, riparian areas, greenways, trails, community gardens, street trees, and nature conservation areas, as well as private backyards and corporate campuses (Cameron and Hitchmough, 2016; Roy et al., 2012). Thus, in this study, the definition of urban greenspace followed this broad concept that all areas covered by green vegetation were considered as greenspaces.

Additionally, differences in data and methods used to map the distribution of greenspaces contributed to another part of the disagreements among existing studies. Although remotely sensed images via satellites have significantly facilitated green vegetation mapping by providing spatially explicit information (Chen et al., 2017), the different levels of spatial details and classification accuracies will lead to inevitable discrepancies. In order to accurately capture and differentiate complex urban features, optical-image-based greenspace map derived from hard classifiers (i.e., each pixel belongs to the class it most closely resembles) always require images with a spatial resolution of at least 5 m (Franke et al., 2009), since it is quite challenging for medium- or coarse-resolution imageries (e.g., Landsat and MODIS) with insufficient spatial details to provide accurate greenspace mapping for complex urban area. More importantly, information on each pixel is always a mixture of several spectral signals from different land cover types, hard classification methods that group pixels into certain categories of land cover (e.g., vegetation, water, soil, etc.) will further contribute to biases in heterogeneous areas (Zhang et al., 2015). Consequently, images with higher resolution and proper classification methods (i.e., soft classifier) should be utilized for urban greenspace mapping.

Unlike green coverage rate (GCR) or greenspace area per capita (GAC) that just provides a general evaluation of urban greenspace, greenspace exposure considering the spatial heterogeneity of population distribution is regarded as a superior indicator for appraising the rationality of greenspace distribution (Mitchell and Popham, 2008). In terms of datasets, static population datasets such as surveys, censuses, and gridded population maps (e.g., LandScan Global Population, Gridded Population of the World series) are widely applied to characterize the geographic distribution of population and evaluate their ambient environmental factors (Chen et al., 2018). However, people are not stationary, and most of them spent less than fifty percent of their daily time at home or their workplace (Gariazzo et al., 2016). Generally, people move around and are engaged in various out-of-home activities in their daily life while their ambient environments may change (Kwan, 2013, 2018a). This fact implies that human mobility should be considered when assessing residents' exposures to ambient green environment. Due to the rapid development of mobile internet and the popularization of diverse computing platforms (e.g., smartphones) and wearable smart devices, the location-based services (LBS) embedded in most apps (application software) produce vast amounts of location-based services data and make it possible for researchers to access direct records of users' distribution in space and time (Liu et al., 2015). Besides, the associations between the spatiotemporal characteristics of such location records and human mobility have been revealed by several pioneering studies (Dunkel, 2015; Gariazzo et al., 2016). Compared with static population data, geospatial big data can be used as useful indicators to depict the actual dynamic distribution of population (Deville et al., 2014) and have been successfully applied in several studies regarding environmental exposure assessments (Chen et al., 2018; Dewulf et al., 2016; Gariazzo et al., 2016; Kwan, 2018b; Nyhan et al., 2016).

3. Study area and datasets

3.1. Study area

In this study, 290 major cities in China were selected to assess the difference in greenspace between old and new urban areas, based on the city's administrative level and the acreage of old urban area (i.e., larger than 10 km^2). These cities include 4 municipalities directly governed by the central government, 15 sub-provincial cities, 16 provincial capital cities, and 255 prefecture-level cities (Fig. 1). Based on their geographic location and economic development characteristics, these 290 cities were grouped into four regions: East Coast, Central China, Northeast China, and Western China. The population of these 290 cities accounts for 95.08% of the total urban population in China (National Bureau of Statistics of China, 2016), which would help to provide a comprehensive sample size of the urban green environments in China.

3.2. Nighttime light images

Nighttime light images (NTL) have been widely used to identify and extract urban areas as well as monitor urban expansion from regional to global scales (Huang et al., 2015; L. Imhoff et al., 1997; Small et al., 2005; Wei et al., 2014). In this study, two types of nighttime light data (i.e., DMSP-OLS NTL data in 1992 and NPP-VIIRS NTL data in 2015) covering the 290 selected cities were used. All the images were obtained directly from the website of the Earth Observation Group, NOAA (https://www.ngdc.noaa.gov/eog). The DMSP-OLS NTL images used in this work were annual stable-lights images (Version 4). The composite data of 1992 were produced using all the available data received by DMSP satellites F12 during 1992, with a spatial resolution of 30 arc-second (about 1 km). All the light from transient events (e.g., fire, ship lights) were excluded before compositing (Ma et al., 2012). The values of the DMSP-OLS NTL data range from 1 to 63, and zero was assigned to background noise. The NPP-VIIRS NTL images were captured by an improved sensor (Visible Infrared Imaging Radiometer Suite, VIIRS) carried by the weather satellite Suomi NPP. The annual cloud-free composites of 2015 used in this work was also produced using all the available data without transient light. With a spatial resolution of 15 arc-second (about 500 m), these NPP-VIIRS NTL images were capable of providing more detailed information than the DMSP-OSL NTL data (Shi et al., 2014). For the annual composites, interferences from stray light, lunar illumination, and cloud cover were all filtered out, and no-light areas (background) were set to zero.

3.3. Land cover data

The land cover data (LC) produced by the Climate Change Initiative of the European Space Agency, namely ESA-CCI LC, were also utilized as sample data for delineating the spatial extent of urban areas. The ESA-CCI LC is a global landcover product with a spatial resolution of 300 m and was updated annually from 1992 to 2015 (www.esa-landcover-cci.org). This land cover classification

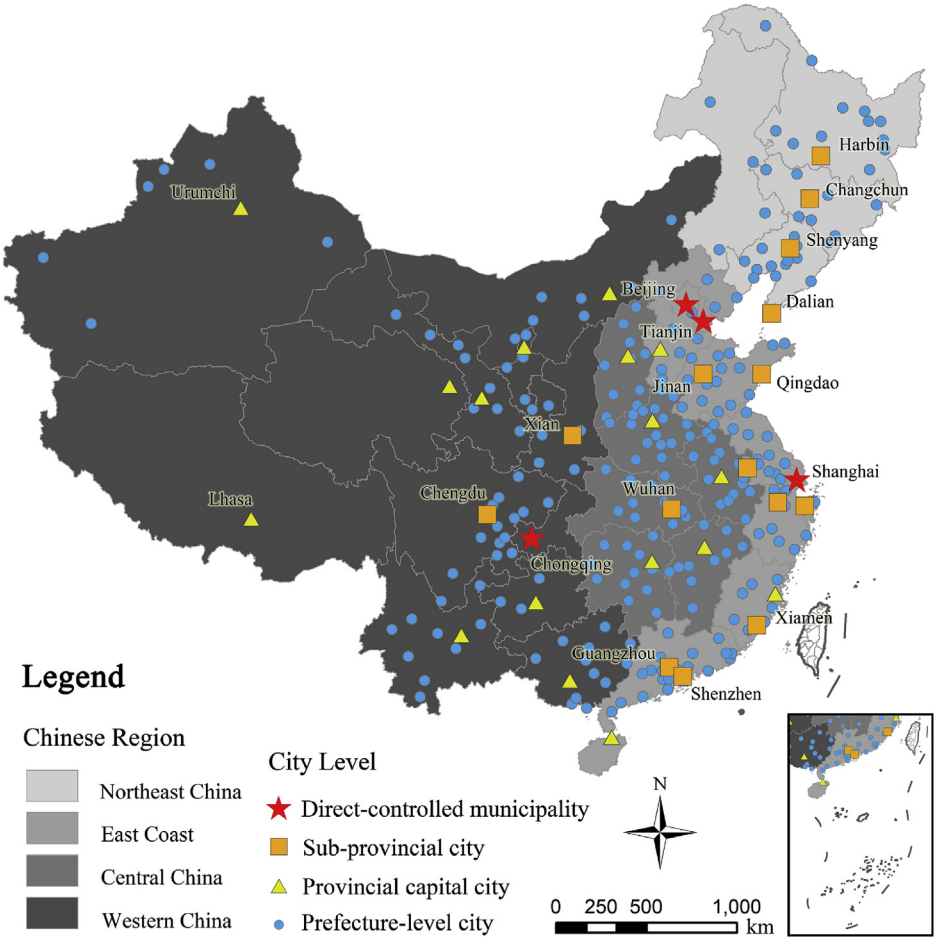

Fig. 1. Distributions of four regions with the forefront selected 290 cities in China.

product was developed based on several earth observation datasets and the GlobCover unsupervised classification chain from the ESA (https://goo.gl/GgA4ei). ESA-CCI LC provides a wealth of landcover information and its overall weighted-area accuracy reaches about 71.1% (Defourny et al., 2009). There were thirty-seven land cover types in ESA-CCI LC data, and the land cover type labeled "urban areas" (i.e., impervious surfaces) in circa years 1992 and 2015 covering China was extracted and used in this study.

3.4. Sentinel-2A image

Launched in June 2015, Sentinel-2A is a sun-synchronous satellite with a 10:30 am descending node and its nominal revisiting time is ten days. It was equipped with Multispectral Instruments (MSI) proving multispectral images with 13 bands, and the spatial resolutions of these bands are diverse (between 10 m and 60 m). The full stack of Sentinel-2A data in 2016 archived in Google Earth Engine were collected, and four bands (Band 2: blue, Band 3: red, Band 4: green, and Band 8: near infrared) of Sentinel-2A images with the same spatial resolution of 10 m were finally used for urban greenspace mapping.

3.5. Mobile phone location-based services big data

Mobile phone location-based services data (LBSD) from Tencent was used to portray the spatiotemporal variation in population distribution and measure people's exposures to urban greenspace during different temporal periods of a day. All the location data were produced by recording real-time locations of active mobile phone users when they are using the apps of Tencent or other mobile apps with a built-in Tencent's location-based service. It should be noted that all information about users' identities and other private information was deleted before the data was released. Given the widespread use of Tencent's popular apps (e.g., WeChat, QQ, Tencent Map) and its location-based services, the daily LBS records from the 450 million of Tencent service users reached over 38 billion globally in 2016 (Tencent, 2016). The data were finally released in raster form with a spatial resolution of approximately 1.2 km and a 5-min update frequency, and all the records produced in 2016 were collected via the Tencent Location Big Data API (https://heat.qq.com).

4. Methods

4.1. Definition of urban boundaries in 1992 and 2015

Generally, there is no clear demarcation between old and new urban areas. New urban areas are usually defined as the newly expanded parts of an urban area while old urban areas refer to the earlier or original parts (Hennig et al., 2015). In this study, urban areas that existed in 1992 were defined as old urban areas, while urban areas that emerged from 1992 to 2015 were defined as new urban areas.

Land cover classification data like ESA-CCI LC can well delineate the extent of different land cover categories. However, areas labeled "urban areas" in such optical-image-based products mainly refer to impervious surfaces or built-up areas (Weng, 2012), but some frequently accessed greenspaces located within or around urban areas (e.g., central parks, forest gardens) were classified as grassland, shrubbery, or woodland. In other words, if we directly use the "urban areas" of some land cover produces like ESA-CCL LC, certain parts of greenspaces where people often visit would be excluded. Therefore, the boundaries of land-cover-based urban areas should be extended to incorporate more frequently accessed spaces into the subsequent assessment and analysis. Given the capabilities of nighttime light (NTL) images in mapping human activities, DMSP-OLS NTL data in 1992 and NPP-VIIRS NTL data in 2015 were then used to implement this task. Using ESA-CCL LC as sample data, a more appropriate spatial extent for greenspace assessment was extracted from nighttime light images through the method presented in Fig. 2a, and the detailed information regarding the methodology was given in Section 1 of the Supplementary Materials. Two methods (i.e., POIs-based and land-cover-based) were then used to evaluate the performance of the proposed method (see Section 2 in the Supplementary Materials), and the plausible producer's accuracies (>92.2%) and overall weighted-area accuracies (>94.6%) illustrated the newly defined urban boundaries were with a high-level confidence. Taking Shenzhen city as an example (Fig. 2b), the NTL-based urban boundaries (red boundaries) surround the "urban area" from ESA-CCL LC data (within blue boundaries) as a buffer, which means that the newly defined urban boundaries could incorporate more frequently-visited spaces and enable some important urban greenspace (e.g., center park, peri-urban areas, and urban forest) to be included in the following analysis. Statistically, compared with the total coverage of the urban areas of the 290 selected cities derived from ESA-CCL LC data (1992: 27205 km^2, 2015: 88465 km^2), the coverage of the NTL-based urban areas was about twice as big (1992: 51309 km^2, 2015: 184786 km^2).

Subsequently, expansion rate (i.e., the proportion of new urban areas in 2015) was defined as:

$$NUAR = \frac{NU}{U_{2015}} \times 100\% \quad (1)$$

$$NU = U_{2015} - U_{1992} \quad (2)$$

where U_{1992} and U_{2015} represent the urban area in 1992 and 2015, respectively.

4.2. Urban greenspace mapping

Considering the widely existing mixed pixels due to heterogeneous and complex urban environments, a linear spectral unmixing model (LSU) (Weng et al., 2004) was adopted to unmix the Sentinel-2A data and produce a fraction map for urban greenspace distribution (see Section 3 in the Supplementary Materials for more information regarding LSU). Using cloud mask and quality assessment (QA) information in the Sentinel-2A metadata, a pixel-based quality check was first conducted to exclude those bad observations contaminated by clouds and shadows from the year-round Sentinel-2A data. To enhance the accuracy of greenspace mapping, *NDVI* (Eq. (3)) as a thematic index-derived band was added to the originally selected four bands of Sentinel-2A (i.e., Band 2–4, Band 8).

$$NDVI = \frac{(NIR - Red)}{(NIR + Red)} \quad (3)$$

Subsequently, we combined the year-round Sentinel-2A imagery to generate the maximum NDVI composite (i.e., the greenest composite), and the composites of the other four selected bands were also produced using the created maximum NDVI band as a per-pixel ordering function. A widely used three-endmember linear mixing model was then adopted for urban greenspace mapping, namely impervious area, water, and vegetation. Sampled pure pixels representing each endmember were then selected from Sentinel-2A images by visual interpretation and inspection with the help of high-spatial-resolution (0.5–1 m) satellite images from Google Earth. Finally, we evaluated the accuracy using another

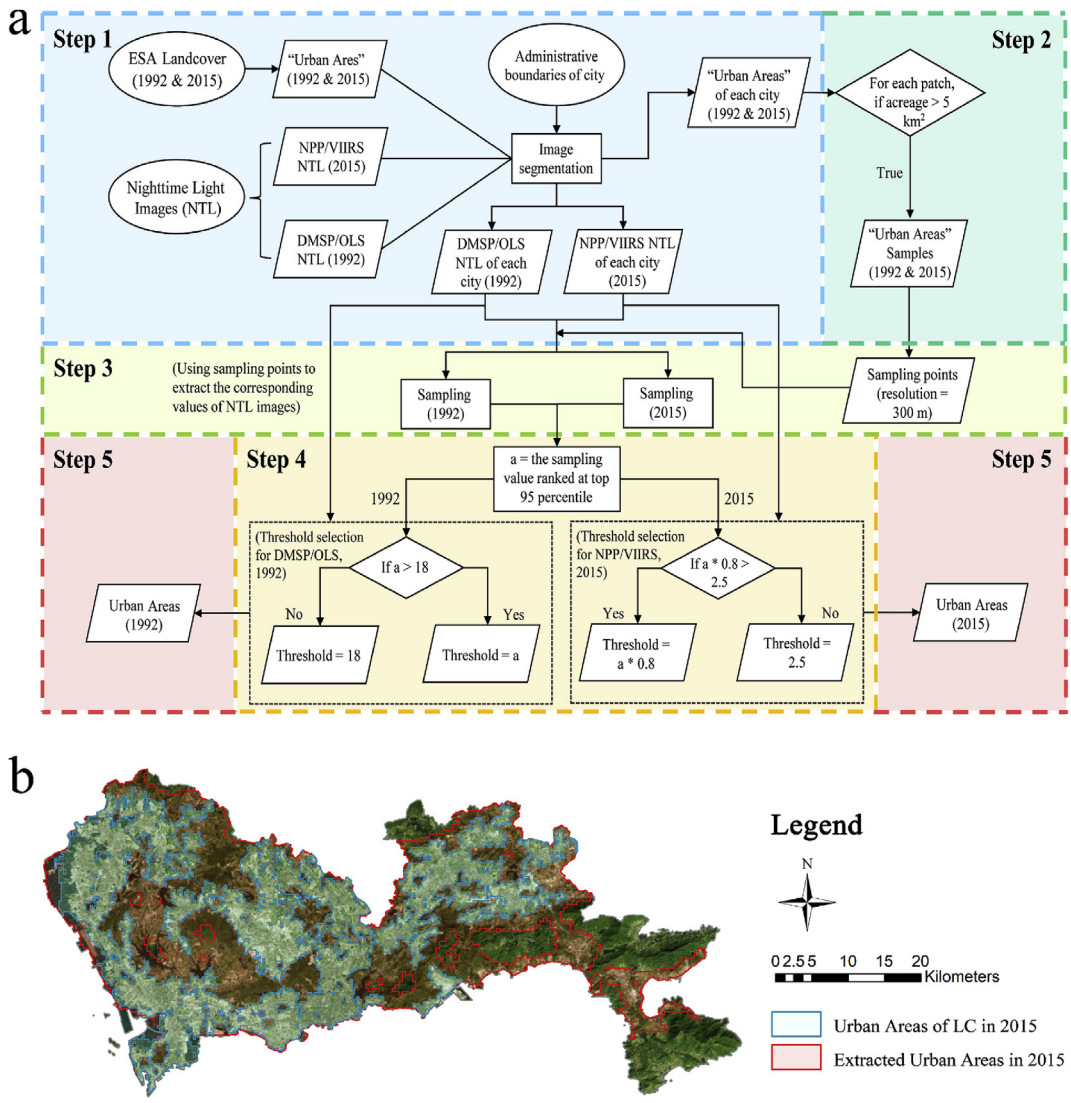

Fig. 2. (a) Flowchart of urban boundaries definition; (b) Comparison of urban areas from ESA-CCL LC data (within the blue boundaries) and NTL-based urban boundaries (red boundaries) extracted by the proposed method: an example of Shenzhen city. (For interpretation of the references to color in this figure legend, the reader is referred to the Web version of this article.)

satellite-based greenspace map with a very high resolution of 1 m (see Section 4 in the Supplementary Materials), and the average correlation coefficient of 0.92 verified the reliability of the Sentinel-2A-based greenspaces maps derived from the linear spectral unmixing model.

The green coverage rate (GCR) of an area can be directly calculated by averaging all corresponding pixels of the Sentinel-2A-based greenspace map within the area. The GCR-based comparisons between old and new urban areas were then made through:

$$D_{old/new} = G_{old}/G_{new} \tag{4}$$

where G_{old} and G_{new} denote the GCR in old and new urban areas respectively, $D_{old/new}$ is their ratio. Specifically, a $D_{old/new}$ larger than 1 indicates that the green coverage rate in old urban areas is higher than that in new urban areas. On the contrary, a $D_{old/new}$ less than 1 means that the green coverage rate in new urban areas is higher.

4.3. LBSD-based greenspace exposure assessment

In this study, greenspace exposure is assessed based on the greenspace coverage rate within a given radius (i.e., 0.6 km) of people's location. Therefore, a model for assessing the average level of population exposure to ambient greenspace within an area (GE) can be defined as Eq. (5).

$$GE = \frac{\sum_{i=1}^{n} G_i}{n} \tag{5}$$

where n denotes the population size within an urban area, G_i is green coverage rate (GCR) within a given radius (i.e., 0.6 km) of the ith person's location.

Given the temporally varying population distribution, the time-series gridded LBSD were utilized to identify people's location during different temporal periods. Due to the lack of information about users' precise positions in each pixel, we assumed that all the people within a pixel are at the center point of the pixel. Therefore, by integrating the pixel-based population distribution information, the average level of population exposure to ambient greenspace

within an area (i.e., *GE*) in Eq. (5) was further modified in a population-weighted manner as shown in Eq. (6):

$$GE = \frac{\sum_{i=1}^{n}(p_i \times G_i)}{\sum_{i=1}^{n} p_i} \quad (6)$$

where p_i represents the population size in the ith grid, and G_i denotes the green coverage rate within the ith grid.

To be specific, the 5-min time-series LBSD was first aggregated into hourly data to reduce computational costs. By averaging the hourly *GE*, the average level of population exposure to ambient greenspace within an area (*GE*) for the whole day (0:00 a.m.–24:00 p.m.), daytime (06:00 a.m. –18:00 p.m.) and nighttime (18:00 p.m.–06:00 a.m.) can be derived.

5. Results

5.1. Urban expansion

Based on the urban boundaries derived from ESA CCI land cover classification data and nighttime light images, rapid urban expansion in China from 1992 to 2015 was identified (Fig. 3a–b). The new urban areas that emerged during this period accounted for a substantial proportion of the entire urban area in 2015, and the average expansion rate of the 290 cities (i.e., NUAR) estimated by Eqs. (1) and (2) was as high as 68.09%. As shown in Fig. 3c, cities at different administrative levels experienced different expansion magnitudes. Prefecture-level cities had the highest average expansion rate of 68.67%, which exceeded the total average rate of all selected cities. Among the 255 prefecture-level cities, 69 cities had expansion rates exceeding 80%, while 16 cities had lower expansion rates of less than 40%. In contrast, the average expansion rates of cities at the other three administrative levels were all less than the overall average rate, and they were 66.35% (provincial capital cities), 62.62% (sub-provincial cities) and 59.19% (municipalities). In terms of the four regions in China (Fig. 3d), the cities located in western China witnessed the highest expansion rate (average rate = 74.43%). The cities in central and eastern China also had relatively high expansion rates of 72.36% and 68.64%, respectively. But the average expansion rate of the cities located in northeast China was much lower (46.02%).

5.2. Greenspace in old and new urban areas

The green coverage rate (GCR) was first estimated for the entire urban area in 2015 for each city. As shown in Fig. 4a, the colored circles stand for the magnitudes of GCR, with darker circles (e.g., dark blue circles) representing higher GCR and lighter circles (e.g., pale yellow circles) representing lower GCR. Note that some cities had a relatively lower greenspace coverage rate, such as the two cities with the lowest GCR were Jinchang (18.18%) and Karamay (16.48%) (Fig. 4a). Statistically, the average GCR for the selected 290 cities was 45.03%, and 11.7% of the 290 cities had a GCR of under 35% (Fig. 4b). In terms of the four regions in China, cities located in Northeastern China and Central China had higher green coverage rate than those located in the East Coast and Western China (Fig. 4c).

The differences in GCR between old and new urban areas were identified as shown in Fig. 5. Taking the city of Harbin as an example (Fig. 5a), an obvious greener "circle-ring" associated with

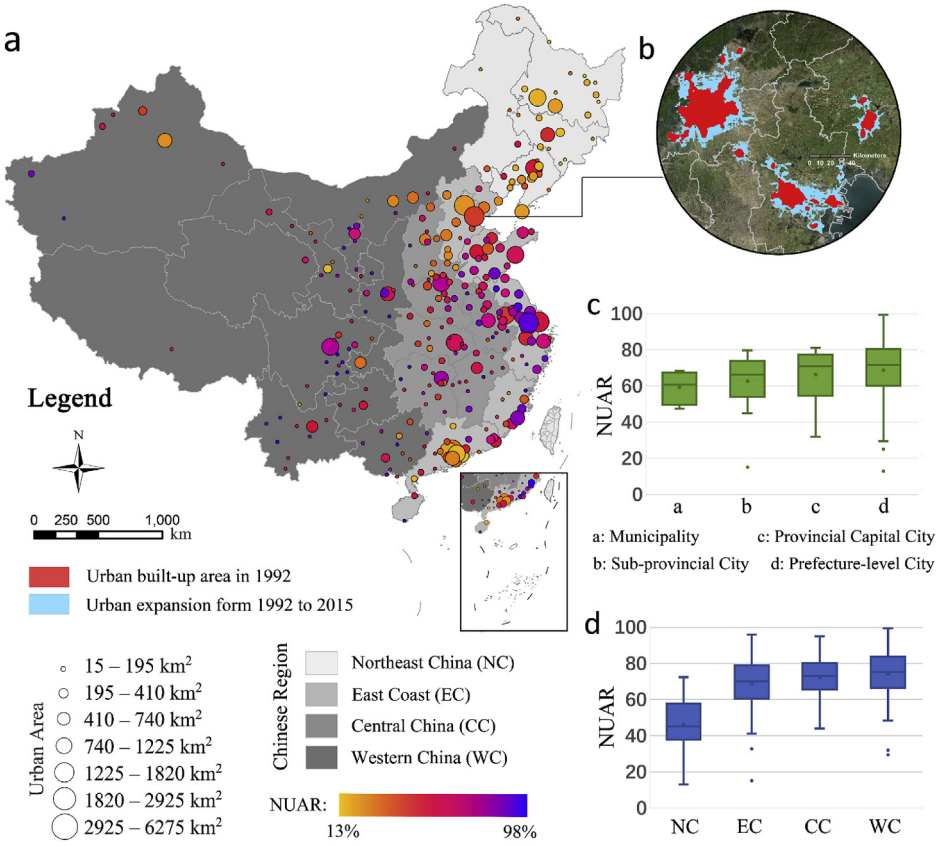

Fig. 3. Urban expansion among the 290 selected cities in China: (a) expansion rate and total urban area in 2015; (b) urban expansion from 1992 to 2015 around Beijing-Tianjin-Hebei region; (c) whisker plot of expansion rate of cities at four administrative levels; (d) whisker plot of expansion rate in the four regions of China.

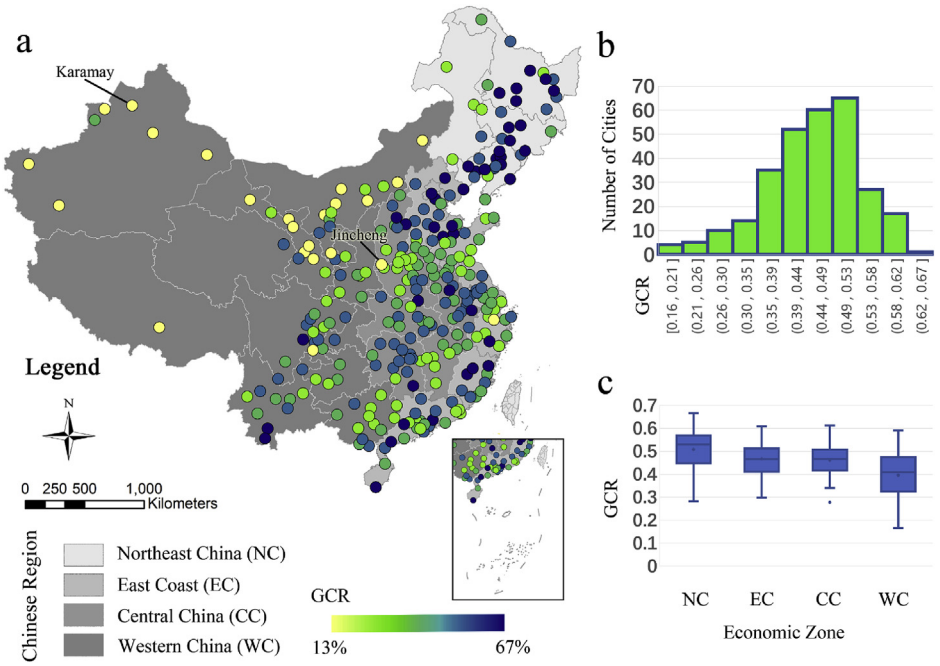

Fig. 4. (a). Green coverage rate (GCR) of the 290 selected Chinese cities' urban areas in 2015; (b). statistical distribution of the cities' GCR values; (c). whisker plot of the cities' GCR values in the four regions of China. (For interpretation of the references to color in this figure legend, the reader is referred to the Web version of this article.)

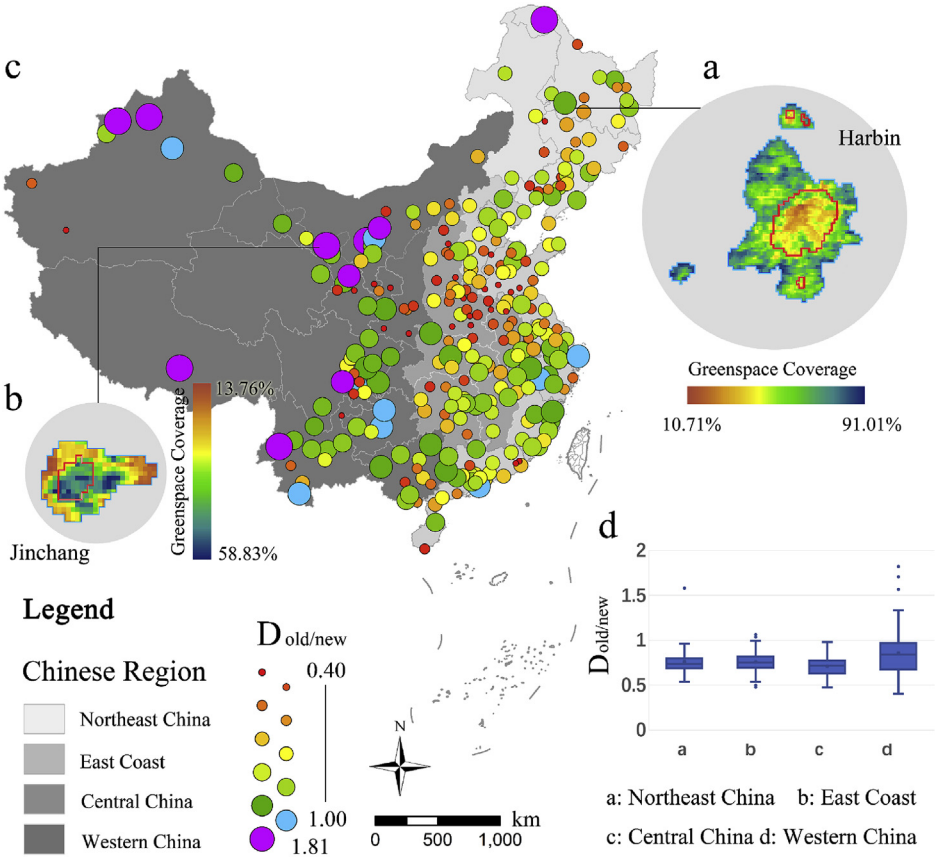

Fig. 5. Differences between old and new urban areas assessed by green coverage rate (GCR): (a–b). greenspace coverage maps of Harbin and Jinchang, respectively. (We resampled the original green coverage map from 10 m to 500 m for visualization); (c). GCR-based $D_{old/new}$ of the 290 selected cities; (d). whisker plot of GCR-based $D_{old/new}$ in the four China regions. (For interpretation of the references to color in this figure legend, the reader is referred to the Web version of this article.)

its new urban areas could be found (the area between the red and blue boundaries in Fig. 5a). To be specific, the GCR of Harbin's old

urban area was 48.65% while it was 69.50% for its new urban areas, thus leading to a relatively lower GCR-based $D_{old/new}$ (0.7). Additionally, the small circles with red, orange, yellow and green colors spreading across the majority of the selected cities in Fig. 5c indicated that these cities were facing similar situations as Harbin (GCR-based $D_{old/new} < 1$). That is, the new urban areas in these cities were having higher GCR when compared with the old urban areas. As for the city of Jinchang (Fig. 5b), an opposite situation was identified, where higher green coverage rate was found in its old urban area (leading to a GCR-based $D_{old/new} > 1$). In addition to Jinchang, we could also identify some other cities experiencing a similar situation (purple circles in Fig. 5c), and almost all of them were in western China. In terms of the regions in China, the largest differences in greenspace coverage rate between old and new urban areas (the lowest average GCR-based $D_{old/new}$ values) appeared in Central China ($D_{old/new} = 0.705$), followed by the East Coast ($D_{old/new} = 0.753$), Northeast China ($D_{old/new} = 0.759$) and Western China ($D_{old/new} = 0.851$) (Fig. 5d). Overall, new urban areas had higher rates of greenspace coverage (48.91%) than old urban areas (36.85%) in the 290 selected cities in China, with a GCR-based $D_{old/new} = 0.768$.

5.3. Greenspace exposure

Based on the mobile-phone LBSD and the greenspace coverage map derived from Sentinel-2A data, the population means of greenspace exposure (GE) during different periods (whole day: GE, day time: GE_{day}, night time: GE_{night}) were computed separately for each city's old and new urban areas, using the method described in Section 4.3.

The differences between GCR and GE, namely (GCR - GE), could help us understand the impact on urban greenspace evaluation when spatiotemporal heterogeneity of population distribution was considered. Fig. 6a–b presented the comparisons (GCR - GE) of old and new urban areas in each selected city. As shown in Fig. 6a, in almost all old urban areas of the cities, the value of GE was lower than that of the GCR (i.e., GCR - GE < 0). Taking the city of Suihua for an instance, the GCR of its old urban area was 49.32%, but its corresponding GE was estimated to be much lower (20.08%). Similar situations were also found in the old urban areas of several cities, such as Shanwei and Songyuan (Fig. 6a), and the new urban areas of some cities, such as Weihai, Ningbo, and Zhongshan (Fig. 6b). However, we only identified limited opposite situations (i.e., GCR - GE > 0) in the old urban areas of seven cities (e.g., Karamay, Lincang, Hechi) and the new urban areas of four cities (e.g., Jiayuguan, Karamay, Fangchenggang). Statistically, the average GE of old and new urban areas for the 290 cities was 25.36% and 35.63%, respectively, which were both lower than the corresponding GCR (old areas: 36.86%, new areas: 48.91%). These generally lower GE indicated that, in the vast majority of Chinese cities, the average greenspace coverage rate of residents' ambient environment was actually lower than the overall rate of the corresponding urban area. That is, more green vegetation was located in the places far away from people.

In addition, the comparison between old and new urban areas based on GE could be conducted in the same way introduced in Section 4.2, as $D_{old/new} = GE_{old}/GE_{new}$, and the results were shown in Fig. 6c. Note that, when the spatiotemporal heterogeneity of population distribution was taken into consideration for the assessment, the differences in urban greenspace between old and new urban areas also changed accordingly. Specifically, compared with the results based on GCR, more cities with GE-based $D_{old/new} > 1$ emerged (purple circles in Fig. 6c), and most of them were also located in Western China. Besides, in terms of different regions in China, the region with the lowest average GE-based $D_{old/new}$ was Northeast China ($D_{old/new} = 0.621$), followed by Central China ($D_{old/new} = 0.675$), the East Coast ($D_{old/new} = 0.718$), and Western China ($D_{old/new} = 0.843$) (Fig. 6d). In the meantime, the average GE-based $D_{old/new}$ of all these four regions were smaller than the corresponding results of GCR-based $D_{old/new}$, which means that the disagreement between old and new urban areas was amplified when the evaluation was conducted based on greenspace exposure.

5.4. Dynamic change of greenspace exposure

People are exposed to different green environments as they move around throughout the day, which would inevitably change the GE in old or new urban areas during different temporal periods. As shown in Fig. 7a, for the old urban areas of many cities, the greenspace exposure in daytime was higher than that during nighttime (i.e., GE_{day} - $GE_{night} > 0$), such as the cities of Dali, Yangjiang, and Liaoyuan. Similar results could also be found in the new urban areas in cities like Dandong, Sanya, and Kashgar (Fig. 7b). Statistically, the old urban areas in 84 of the 290 cities had higher GE_{day}, while the new urban areas in 137 cities had high GE_{day}. The average GE_{day} of the old and new urban areas were 25.25% and 35.59%, respectively; and the average GE_{night} of the old and new urban areas were 25.51% and 35.67%, respectively. The difference between GE_{day} and GE_{night} (i.e., GE_{day} - GE_{night}) for urban area indicated that human mobility did have a significant impact on people's ambient green environment and thus change the value of GE-based $D_{old/new}$ of a city during different periods (Table S6 in the Supplementary Materials).

6. Discussion

Urbanization directly led to the difference in green environment between the old and new urban areas in Chinese cities. These differences were not only observed using the general evaluation index as green coverage rate (i.e., GCR-based $D_{old/new}$) but also captured by the LBSD-based greenspace exposure (i.e., GE-based $D_{old/new}$). Except for a few cities that are mainly located in Western China, new urban areas of most Chinese cities had better green environments (i.e., higher green coverage rate or greenspace exposure level) than their corresponding old urban areas. The emerging "greener" new urban areas could be attributed to a number of factors, for example, the favorable natural endowment, the low intensity of land development, and the positive policy-driven intervention. It should be noted that the pleasant environment in new urban areas were likely to draw more people to live, which would increase both rural-urban and inter-city migrations. However, when lots of people moved to the new urban areas for better green environments, old urban areas would become unvital and even begin to degenerate (Deng and Ma, 2015). Meanwhile, the migration-induced increase of population density in new urban areas might also give rise to or accelerate some emerging environmental issues, such as air pollution, noise pollution, and greenspace degradation (Chen et al., 2017; Han et al., 2014; McMahon et al., 2017; Wei et al., 2019), which undoubtedly intimidate the sustainable development of city.

Obvious regional discrepancies in GCR-based $D_{old/new}$ and GE-based $D_{old/new}$ were also observed in China. This type of regional difference could be caused by the geographical, climatic, and socioeconomic features of different regions. For example, the ideal physical and climatic conditions in northeast China contribute to favorable ecological natural environments surrounding urban areas. At the same time, profit-oriented land finance of local governments in recent years (i.e., a type of fiscal revenue strategy based on land grant premiums and related tax revenues) has accelerated urban sprawl (Cao et al., 2008; Qun et al., 2015) but low

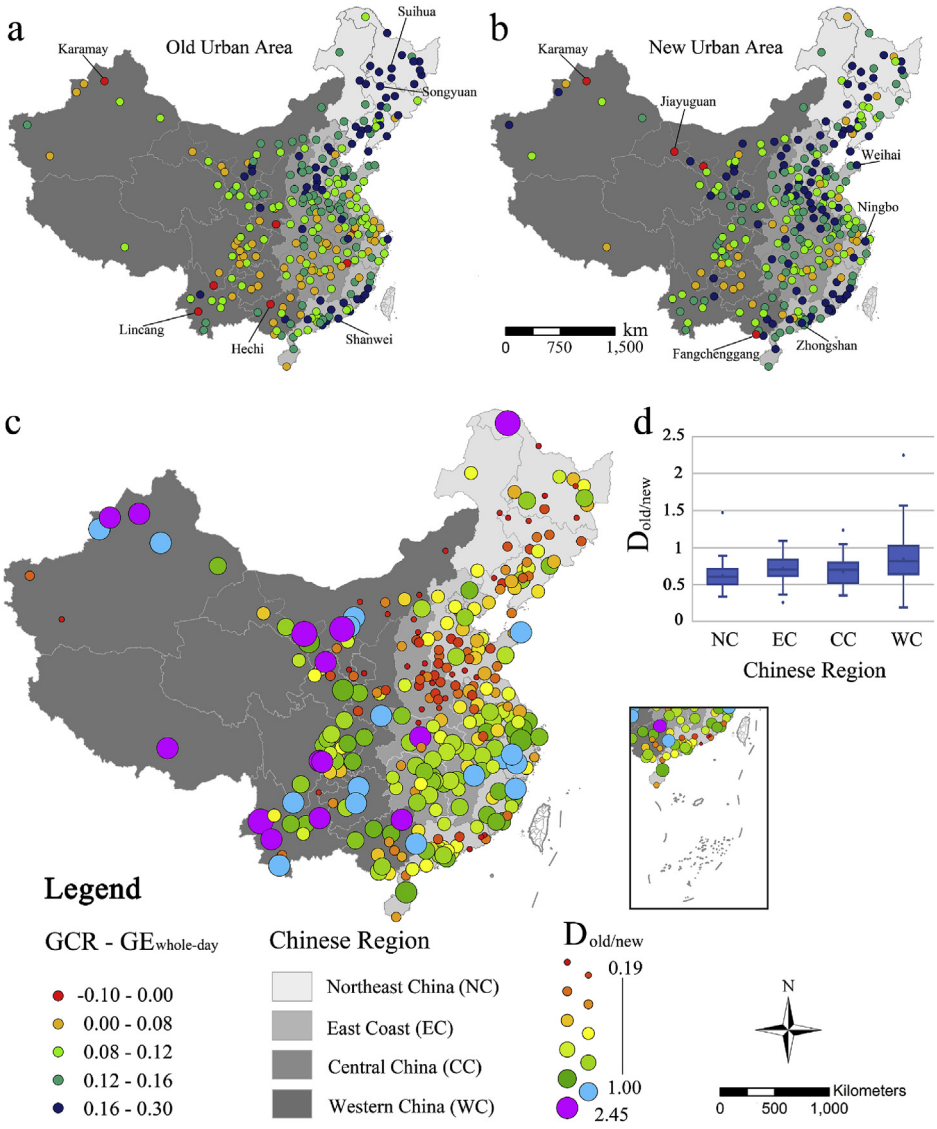

Fig. 6. (a–b) Comparison of green coverage rate and greenspace exposure (i.e., GCR - GE) in old and new urban areas, respectively; (c). GE-based $D_{old/new}$ values of the 290 selected cities; (d). whisker plot of GE-based $D_{old/new}$ in the four Chinese regions. (For interpretation of the references to color in this figure legend, the reader is referred to the Web version of this article.)

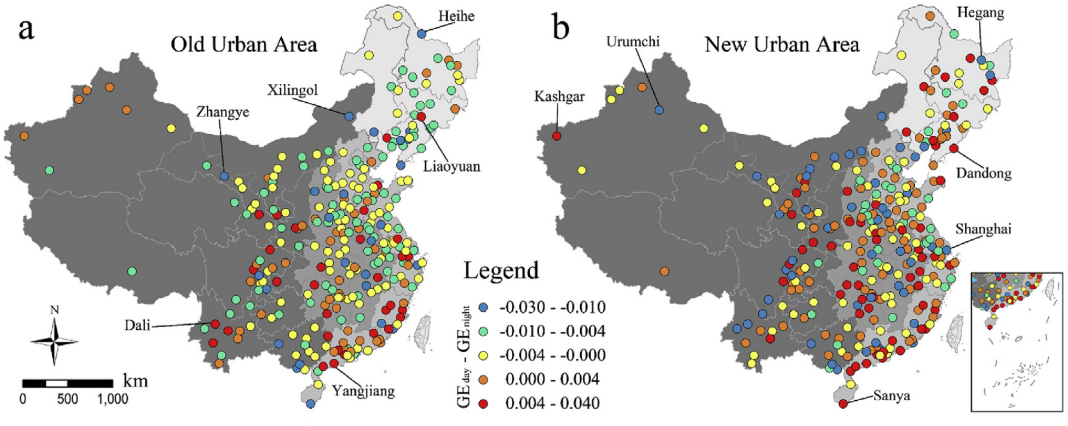

Fig. 7. Comparisons of GE_{day} and GE_{night} (GE_{day} - GE_{night}) in old (a) and new (b) urban areas.

land-use intensity (Long and Gao, 2019). It means that a considerable part of new urban area would remain its original land cover type (mainly for grassland and woodland). Therefore, this extensive development pattern may ultimately result in the significantly higher greenspace exposure level of new urban areas in the cities of northeast China (i.e., lowest average GE-based $D_{old/new}$). Besides, the lack of policy and financial support from the local governments may also hinder the construction of greenspace in old urban areas (Byomkesh et al., 2012), thus further enlarging the differences between old and new urban areas.

Our results also demonstrate that urbanization did not always negatively impact on the urban green environment, especially in regions with harsh natural conditions, which is opposite to that of some other works (Zhao et al., 2013; Zhou and Wang, 2011). Cities located in western China generally had semiarid/arid climates or desert climates, characterized with low precipitation (less than 400 nm), and significant seasonal differences in temperature, thus leading to less dense vegetated areas in these areas compared with eastern China. However, the willingness to live in a greener environment prompts people to make every endeavor to improve this undesirable situation (e.g., planting more trees, irrigating urban greenery). This finding can be used to explain why, in some cities in the arid regions of western China, highly urbanized old urban areas had better green coverage rates than their adjacent newly expanded parts (i.e., GCR-based $D_{old/new} > 1$). Moreover, compared with GCR-based $D_{old/new}$, the relatively larger GE-based $D_{old/new}$ in some of these western cities indicated that more green vegetations were artificially put in the places near people.

An excellent urban green environment is the ultimate goal of urban development, but it cannot be realized without the support of the government. Active policy and encouragement from the government have been considered as one of the most important factors for urban greenspace improvement and construction (Maas et al., 2006; Zhou and Wang, 2011). Over the past three decades, several policies and standards had been issued by the central government of China, such as the Regulations of Urban Greening (1992), Standards of National Garden City (2000, 2005, 2010). All these guidelines set strict standards to ensure the quantity and quality of urban greenspace during the process of urbanization in China. However, as presented in above results, the principle of a balanced development is not adequately addressed in practicing these standards, thus leading to an obvious difference in greenspace supply among different urban areas. Accordingly, reasonable and sustainable urban greenspace construction with comprehensive schemes considering the equitable development in both old and new urban areas are essential for the future urban development in China.

In addition, the assessment based on greenspace exposure presents a better way for urban greenspace analysis. Traditional evaluation methods can only provide a general evaluation for whole study areas but ignore the dynamic interaction between people and their environmental contexts. The significant differences between the green coverage rate and greenspace exposure in both old and new urban areas not only reveal that most of the urban greenspaces were far away from their residents but also indicated that traditional static evaluations could not provide accurate assessments of people's exposures to ambient green environment. The limitations of static data and methods have been discussed in many urban planning and environmental health and geographic studies (Kwan, 2012, 2013). Kwan (2012) articulated this issue as part of the uncertain geographic context problem (UGCoP), which highlights that delineations of the geographic and temporal contexts of people's environmental exposures can have a significant influence on the research conclusions about the effects of environmental influences. This problem arises when the exposure assessments were conducted using static administrative areal units (e.g., census tracts) which cannot accurately capture individuals' exact location in space and time (Kwan, 2018a, b; Park and Kwan, 2017). Further, specific statistical biases (neighborhood effect averaging) in exposure assessments may also arise due to the neglect of individual mobility (Kwan, 2018a). Therefore, the LBSD-based dynamic assessment used in this study proposed a practical solution to these problems to some extent.

Meanwhile, some potential biases and limitations in this study should be pointed out. Geospatial big data (e.g., cellular signaling records, social media posts, public transit card transactions, points of interest (POIs), and location-based service (LBS) data from smartphone apps) are regarded as non-representative data (Kwan, 2016; Zagheni and Weber, 2015). This kind of data tend to leave out some sections of the society (e.g., children, the elderly, and the poor) since a lower proportion of these people use mobile phones when compared to society at large. We should thus remain cautious about the results and conclusions obtained using these data. Besides, the urban boundaries derived from NTL images maybe leave out a fraction of areas with high-level human activity but low-level nighttime light. But the satisfactory POI-based producer accuracy illustrated that the NTL-based urban boundaries could include the vast majority of the areas with dense human activities.

7. Conclusions

This study sought to use Sentinel-2 derived greenspace coverage and mobile-phone location-based service big data to provide a comprehensive comparison of urban greenspace between the old and new urban areas in 290 Chinese cities. Our results showed the rapid urban expansion from 1992 to 2015 had led to large differences in green environments between old and new urban areas in China. These differences were both captured by the general evaluation index as green coverage rate and the dynamic assessment of people's exposure to greenspace. Generally, for most of China's large cities, people could enjoy more greenspace in new urban areas than in old urban areas, except for a few cities located in Western China. Additionally, we also identified significant day-to-night variations of people's exposure to greenspace between old and new urban areas, which provided new insights about how people were exposed to different green environments when they moved around throughout a day. The measurements and comparisons provided in this work would help us better understand the differences and changes in people's ambient greenspace during rapid urbanization and offered potential utilities for improving our nearby living environment as well as lessening environmental inequality.

Acknowledgements

This work was supported by the Ministry of Science and Technology of China under the National Key Research and Development Program (2016YFA0600104) and by Open Projects Fund of Shanghai Key Laboratory of Urban Renewal and Spatial Optimization Technology (2019030310), and by donations from Delos Living LLC and the Cyrus Tang Foundation to Tsinghua University. The authors thank two anonymous reviewers and the editor for providing valuable suggestions and comments, which are greatly helpful in improving the manuscript. The anthors also thank Tencent for making the LBS data publicly available.

Appendix A. Supplementary data

Supplementary data to this article can be found online at https://doi.org/10.1016/j.jclepro.2019.119018.

References

Akpinar, A., 2016. How is quality of urban green spaces associated with physical activity and health? Urban For. Urban Green. 16, 76–83.

Andersson-Sköld, Y., Thorsson, S., Rayner, D., Lindberg, F., Janhäll, S., Jonsson, A., Moback, U., Bergman, R., Granberg, M., 2015. An integrated method for assessing climate-related risks and adaptation alternatives in urban areas. Climate Risk Management 7, 31–50.

Byomkesh, T., Nakagoshi, N., Dewan, A.M., 2012. Urbanization and green space dynamics in Greater Dhaka, Bangladesh. Landsc. Ecol. Eng. 8, 45–58.

Cameron, R., Hitchmough, J., 2016. Environmental Horticulture: Science and Management of Green Landscapes. Cabi.

Cao, G., Feng, C., Tao, R., 2008. Local "land finance" in China's urban expansion: challenges and solutions. China World Econ. 16, 19–30.

Chen, B., Nie, Z., Chen, Z., Xu, B., 2017. Quantitative estimation of 21st-century urban greenspace changes in Chinese populous cities. Sci. Total Environ. 609, 956–965.

Chen, B., Song, Y., Jiang, T., Chen, Z., Huang, B., Xu, B., 2018. Real-time estimation of population exposure to $PM_{2.5}$ using mobile- and station-based big data. Int. J. Environ. Res. Public Health 15 (4), 573.

Chen, B., Song, Y., Kwan, M., Huang, B., Xu, B., 2018. How do people in different places experience different levels of air pollution? using worldwide Chinese as a lens. Environ. Pollut. 238, 874–883.

Defourny, P., Schouten, L., Bartalev, S., Bontemps, S., Cacetta, P., De Wit, A., Di Bella, C., Gérard, B., Giri, C., Gond, V., 2009. Accuracy Assessment of a 300 M Global Land Cover Map: the GlobCover Experience.

Deng, C., Ma, J., 2015. Viewing urban decay from the sky: a multi-scale analysis of residential vacancy in a shrinking U.S. city. Landsc. Urban Plan. 141, 88–99.

Deville, P., Linard, C., Martin, S., Gilbert, M., Stevens, F.R., Gaughan, A.E., Blondel, V.D., Tatem, A.J., 2014. Dynamic population mapping using mobile phone data. Proc. Natl. Acad. Sci. 111, 15888.

Dewulf, B., Neutens, T., Lefebvre, W., Seynaeve, G., Vanpoucke, C., Beckx, C., Van de Weghe, N., 2016. Dynamic assessment of exposure to air pollution using mobile phone data. Int. J. Health Geogr. 15, 14.

Dunkel, A., 2015. Visualizing the perceived environment using crowdsourced photo geodata. Landsc. Urban Plan. 142, 173–186.

Ernstson, H., 2013. The social production of ecosystem services: a framework for studying environmental justice and ecological complexity in urbanized landscapes. Landsc. Urban Plan. 109, 7–17.

Franke, J., Roberts, D.A., Halligan, K., Menz, G., 2009. Hierarchical multiple endmember spectral mixture analysis (MESMA) of hyperspectral imagery for urban environments. Remote Sens. Environ. 113, 1712–1723.

Fuller, R.A., Gaston, K.J., 2009. The scaling of green space coverage in European cities. Biol. Lett. 5, 352–355.

Fulton, W.B., Pendall, R., Nguyẽ^n, M., Harrison, A., 2001. Who Sprawls Most?: How Growth Patterns Differ across the US. Brookings Institution, Center on Urban and Metropolitan Policy, Washington, DC.

Gariazzo, C., Pelliccioni, A., Bolignano, A., 2016. A dynamic urban air pollution population exposure assessment study using model and population density data derived by mobile phone traffic. Atmos. Environ. 131, 289–300.

Giles-Corti, B., Vernez-Moudon, A., Reis, R., Turrell, G., Dannenberg, A.L., Badland, H., Foster, S., Lowe, M., Sallis, J.F., Stevenson, M., Owen, N., 2016. City planning and population health: a global challenge. The Lancet 388, 2912–2924.

Gong, P., Liang, S., Carlton, E.J., Jiang, Q., Wu, J., Wang, L., Remais, J.V., 2012. Urbanisation and health in China. The Lancet 379, 843–852.

Grimm, N.B., Foster, D., Groffman, P., Grove, J.M., Hopkinson, C.S., Nadelhoffer, K.J., Pataki, D.E., Peters, D.P., 2008. The changing landscape: ecosystem responses to urbanization and pollution across climatic and societal gradients. Front. Ecol. Environ. 6, 264–272.

Han, L., Zhou, W., Li, W., Li, L., 2014. Impact of urbanization level on urban air quality: a case of fine particles (PM2.5) in Chinese cities. Environ. Pollut. 194, 163–170.

He, C., Liu, Z., Tian, J., Ma, Q., 2014. Urban expansion dynamics and natural habitat loss in China: a multiscale landscape perspective. Glob. Chang. Biol. 20, 2886–2902.

Hennig, E.I., Schwick, C., Soukup, T., Orlitová, E., Kienast, F., Jaeger, J.A.G., 2015. Multi-scale analysis of urban sprawl in Europe: towards a European de-sprawling strategy. Land Use Policy 49, 483–498.

Huang, Q., He, C., Gao, B., Yang, Y., Liu, Z., Zhao, Y., Dou, Y., 2015. Detecting the 20 year city-size dynamics in China with a rank clock approach and DMSP/OLS nighttime data. Landsc. Urban Plan. 137, 138–148.

Imhoff, M.L., Lawrence, W.T., Stutzer, D.C., Elvidge, C.D., 1997. A technique for using composite DMSP/OLS "City Lights" satellite data to map urban area. Remote Sens. Environ. 61, 361–370.

Janhäll, S., 2015. Review on urban vegetation and particle air pollution – deposition and dispersion. Atmos. Environ. 105, 130–137.

Jiang, L., O'Neill, B.C., 2017. Global urbanization projections for the shared socioeconomic pathways. Glob. Environ. Chang. 42, 193–199.

Jim, C.Y., Chen, S.S., 2003. Comprehensive greenspace planning based on landscape ecology principles in compact Nanjing city, China. Landsc. Urban Plan. 65, 95–116.

Kong, F., Yin, H., Nakagoshi, N., 2007. Using GIS and landscape metrics in the hedonic price modeling of the amenity value of urban green space: a case study in Jinan City, China. Landsc. Urban Plan. 79, 240–252.

Kwan, M.-P., 2012. The uncertain geographic context problem. Ann. Assoc. Am. Geogr. 102, 958–968.

Kwan, M.-P., 2013. Beyond space (as we knew it): toward temporally integrated geographies of segregation, health, and accessibility. Ann. Assoc. Am. Geogr. 103, 1078–1086.

Kwan, M.-P., 2016. Algorithmic geographies: big data, algorithmic uncertainty, and the production of geographic knowledge. Ann. Assoc. Am. Geogr. 106, 274–282.

Kwan, M.-P., 2018a. The limits of the neighborhood effect: contextual uncertainties in geographic, environmental health, and social science research. Ann. Assoc. Am. Geogr. 108, 1482–1490.

Kwan, M.-P., 2018b. The neighborhood effect averaging problem (NEAP): an elusive confounder of the neighborhood effect. Int. J. Environ. Res. Public Health *15*.

Lang, W., Chen, T., Li, X., 2016. A new style of urbanization in China: transformation of urban rural communities. Habitat Int. 55, 1–9.

Liu, Y., Liu, X., Gao, S., Gong, L., Kang, C., Zhi, Y., Chi, G., Shi, L., 2015. Social sensing: a new approach to understanding our socioeconomic environments. Ann. Assoc. Am. Geogr. 105, 512–530.

Livesley, S.J., McPherson, E.G., Calfapietra, C., 2016. The urban forest and ecosystem services: impacts on urban water, heat, and pollution cycles at the tree, street, and city scale. J. Environ. Qual. 45, 119–124.

Long, Y., Gao, S., 2019. Shrinking Cities in China: the Other Facet of Urbanization. Springer.

Ma, T., Zhou, C., Pei, T., Haynie, S., Fan, J., 2012. Quantitative estimation of urbanization dynamics using time series of DMSP/OLS nighttime light data: a comparative case study from China's cities. Remote Sens. Environ. 124, 99–107.

Maas, J., Verheij, R.A., Groenewegen, P.P., De Vries, S., Spreeuwenberg, P., 2006. Green space, urbanity, and health: how strong is the relation? J. Epidemiol. Community Health 60, 587–592.

McMahon, T.A., Rohr, J.R., Bernal, X.E., 2017. Light and noise pollution interact to disrupt interspecific interactions. Ecology 98, 1290–1299.

Mitchell, R., Popham, F., 2008. Effect of exposure to natural environment on health inequalities: an observational population study. The Lancet 372, 1655–1660.

National Bureau of Statistics of China, 2016. Statistical Communiqué of the People's Republic of China on the 2015 National Economic and Social Development. National Bureau of Statistics of China, Beijing.

Nyhan, M., Grauwin, S., Britter, R., Misstear, B., McNabola, A., Laden, F., Barrett, S.R.H., Ratti, C., 2016. "Exposure track"—the impact of mobile-device-based mobility patterns on quantifying population exposure to air pollution. Environ. Sci. Technol. 50, 9671–9681.

Park, Y.M., Kwan, M.-P., 2017. Individual exposure estimates may be erroneous when spatiotemporal variability of air pollution and human mobility are ignored. Health Place 43, 85–94.

Qun, W., Yongle, L., Siqi, Y., 2015. The incentives of China's urban land finance. Land Use Policy 42, 432–442.

Roy, S., Byrne, J., Pickering, C., 2012. A systematic quantitative review of urban tree benefits, costs, and assessment methods across cities in different climatic zones. Urban For. Urban Green. 11, 351–363.

Shi, K., Huang, C., Yu, B., Yin, B., Huang, Y., Wu, J., 2014. Evaluation of NPP-VIIRS night-time light composite data for extracting built-up urban areas. Rem. Sens. Lett. 5, 358–366.

Sister, C., Wolch, J., Wilson, J., 2010. Got green? Addressing environmental justice in park provision. Geojournal 75, 229–248.

Small, C., Pozzi, F., Elvidge, C.D., 2005. Spatial analysis of global urban extent from DMSP-OLS night lights. Remote Sens. Environ. 96, 277–291.

Tencent, 2016. Tencent Annual Report. Tencent: Shenzhen, China, 2016.

Van Renterghem, T., Botteldooren, D., 2016. View on outdoor vegetation reduces noise annoyance for dwellers near busy roads. Landsc. Urban Plan. 148, 203–215.

Wang, H., He, Q., Liu, X., Zhuang, Y., Hong, S., 2012. Global urbanization research from 1991 to 2009: a systematic research review. Landsc. Urban Plan. 104, 299–309.

Wei, J., Huang, W., Li, Z., Xue, W., Peng, Y., Sun, L., Cribb, M., 2019. Estimating 1-km-resolution PM2. 5 concentrations across China using the space-time random forest approach. Remote Sens. Environ. 231, 111221.

Wei, Y., Liu, H., Song, W., Yu, B., Xiu, C., 2014. Normalization of time series DMSP-OLS nighttime light images for urban growth analysis with pseudo invariant features. Landsc. Urban Plan. 128, 1–13.

Weng, Q., 2012. Remote sensing of impervious surfaces in the urban areas: requirements, methods, and trends. Remote Sens. Environ. 117, 34–49.

Weng, Q., Lu, D., Schubring, J., 2004. Estimation of land surface temperature–vegetation abundance relationship for urban heat island studies. Remote Sens. Environ. 89 (4), 467–483.

Wolch, J.R., Byrne, J., Newell, J.P., 2014. Urban green space, public health, and environmental justice: the challenge of making cities 'just green enough'. Landsc. Urban Plan. 125, 234–244.

Xiao, P., Wang, X., Feng, X., Zhang, X., Yang, Y., 2014. Detecting China's urban expansion over the past three decades using nighttime light data. IEEE J. Select. Top. Appl. Earth Obs. Rem. Sens. 7, 4095–4106.

Yang, J., Huang, C., Zhang, Z., Wang, L., 2014. The temporal trend of urban green coverage in major Chinese cities between 1990 and 2010. Urban For. Urban Green. 13, 19–27.

Zagheni, E., Weber, I., 2015. Demographic research with non-representative internet data. Int. J. Manpow. 36, 13–25.

Zhang, B., Xie, G.-d., Li, N., Wang, S., 2015. Effect of urban green space changes on the role of rainwater runoff reduction in Beijing, China. Landsc. Urban Plan. 140,

8–16.
Zhang, H.K., Roy, D.P., Yan, L., Li, Z., Huang, H., Vermote, E., Skakun, S., Roger, J.-C., 2018. Characterization of Sentinel-2A and Landsat-8 top of atmosphere, surface, and nadir BRDF adjusted reflectance and NDVI differences. Remote Sens. Environ. 215, 482–494.
Zhao, J., Chen, S., Jiang, B., Ren, Y., Wang, H., Vause, J., Yu, H., 2013. Temporal trend of green space coverage in China and its relationship with urbanization over the last two decades. Sci. Total Environ. 442, 455–465.
Zhou, X., Wang, Y.-C., 2011. Spatial–temporal dynamics of urban green space in response to rapid urbanization and greening policies. Landsc. Urban Plan. 100, 268–277.